

Heteronuclear trimetallic and 1D polymeric 3d–4f Schiff base complexes with OCN[−] and SCN[−] ligands†

Shunsheng Zhao,^{a,b} Xingqiang Lü,^b Anxin Hou,^a Wai-Yeung Wong,^b Wai-Kwok Wong,^{*b} Xiaoping Yang^c and Richard A. Jones^{*c}

Received 1st May 2009, Accepted 7th September 2009

First published as an Advance Article on the web 24th September 2009

DOI: 10.1039/b908682j

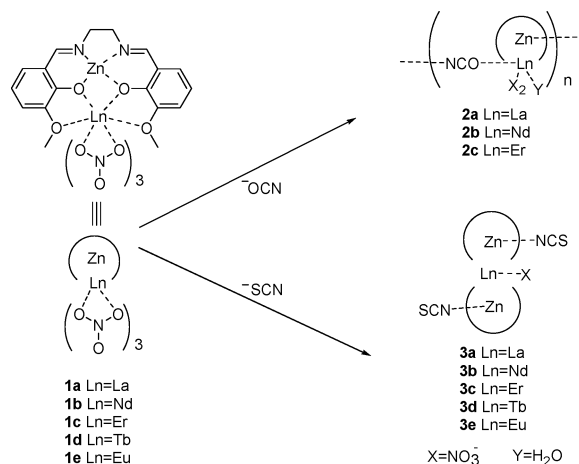
Reactions of heterobimetallic 3d–4f Schiff base complexes of the formula [ZnLnL(H₂O)(NO₃)₃] (**1a–e**) with KOCN or NH₄SCN in refluxing MeCN produce either one dimensional polymeric materials [ZnLnL(NO₃)₂(H₂O)(OCN)]_∞ (**2a–c**) or trinuclear complexes of the formula [Zn₂LnL₂(NO₃)(SCN)₂] (**3a–e**) (**a** (La), **b** (Nd), **c** (Er), **d** (Tb), **e** (Eu); H₂L = *N,N'*-bis-(3-methoxysalicylidene)ethylene-1,2-diamine). The structures of **2a,b** and **3b–e** have been determined by single-crystal X-ray diffraction studies. Structural differences between the complexes affect the photophysical properties, which have been studied in acetonitrile solutions.

Introduction

There is considerable interest in the chemistry of luminescent lanthanide materials due to potential applications in biology,¹ medicine² and materials science.³ For lanthanide ions, because the f–f transitions are parity forbidden, the absorption coefficients are normally very low and the emissive rates are low. Organic ligands, with strongly absorbing chromophores that transfer energy to the lanthanide, can be used to overcome this drawback (antenna effect).⁴ Thus, multidentate cyclic and acyclic ligands such as cryptands, calixarene and cyclodextrins^{4,5} as well as d-block transition metal complexes⁶ that have absorptions in the near UV or visible spectrum have been explored in order to sensitize and enhance the emissive properties of Ln(III) ions.

Our studies have recently focused on the use of various Zn-Schiff base complexes as sensitizers for lanthanide luminescence.⁷ In many cases these 3d–4f heterometallic complexes also bear relatively innocent additional ligands such as acetate (OAc[−]), chloride (Cl[−]) or nitrate (NO₃[−]) which can bind to either the 3d or 4f metal center or both. In other cases, further coordination of the 4f center by solvent molecules such as ROH (R = H, Me or Et) can occur and this can lead to undesirable and partial quenching of the luminescence. Interestingly, the use of multidentate bipyridyl⁷ⁱ or dicarboxylate^{7j} linking groups produces higher polynuclear species or multidimensional network structures in which coordination of solvent molecules is further restricted and this results in enhanced luminescence. Two of the simplest ligands, with potentially dual binding sites, are the linear ions cyanate (OCN[−]) and thiocyanate

(SCN[−]).⁸ These ligands have the potential to bridge between metal centers and create higher nuclearity species. We have therefore investigated the use of both ligands in our heterobimetallic 3d–4f systems and describe here 1D polymeric species, which are formed with cyanate (OCN[−]) and trinuclear Zn₂Ln complexes based on SCN[−] (Scheme 1). The photophysical properties of these complexes in solution are also reported.



Scheme 1 Synthesis of heterometallic 1D polymeric and trimetallic 3d–4f complexes.

Results and discussion

Reaction of the heterobimetallic 3d–4f precursor compounds [ZnLnL(H₂O)(NO₃)₃] (**1**) with potassium cyanate (KOCN) or ammonium thiocyanate (NH₄SCN) in refluxing acetonitrile, followed by filtration and slow evaporation of solution produces analytically pure X-ray quality crystals of the new complexes after several weeks.

Reactions with KOCN produced materials with 1D zig-zag structures of the formula [ZnLnL(NO₃)₂(H₂O)(OCN)]_∞ (**2a–c**), while NH₄SCN gave trinuclear complexes [Zn₂LnL₂(NO₃)(SCN)₂] (**3a–e**; **a** (La), **b** (Nd), **c** (Er), **d** (Tb), **e** (Eu)). IR spectroscopic data

^aCollege of Chemistry and Molecular Sciences, Wuhan University, Wuhan, 430072, Hubei, China.

^bDepartment of Chemistry and Centre for Advanced Luminescence Materials, Hong Kong Baptist University, Waterloo Road, Kowloon Tong, Hong Kong, China. E-mail: wkwong@hkbu.edu.hk

^cDepartment of Chemistry and Biochemistry, The University of Texas at Austin, 1 University Station, A5300, Austin, 78712-0165, TX, USA. E-mail: rajones@mail.utexas.edu

† Electronic supplementary information (ESI) available: ESI-MS data for compounds **2a**, **2b**, **3a** and **3b**. CCDC reference numbers 700787, 700788 and 729274–729277. For ESI and crystallographic data in CIF or other electronic format see DOI: 10.1039/b908682j

Table 1 Crystal data and structure refinement for lanthanide complexes

	2a	2b	3b	3c	3d	3e
Formula	C ₁₉ H ₂₀ N ₅ O ₁₂ ZnLa	C ₁₉ H ₂₀ N ₅ O ₁₂ ZnNd	C ₄₀ H ₃₉ N ₈ O ₁₁ S ₂ Zn ₂ Nd	C ₃₈ H ₃₈ N ₇ O ₁₂ S ₂ Zn ₂ Er	C ₄₀ H ₃₉ N ₈ O ₁₁ S ₂ -Zn ₂ Tb	C ₄₀ H ₃₉ N ₈ O ₁₁ S ₂ -Zn ₂ Eu
FW	714.68	720.01	1146.89	1146.86	1161.57	1154.61
Crystal system	Monoclinic	Monoclinic	Triclinic	Triclinic	Triclinic	Triclinic
Space group	<i>P</i> 2 ₁ / <i>c</i>	<i>P</i> 2 ₁ / <i>c</i>	<i>P</i> $\bar{1}$	<i>P</i> $\bar{1}$	<i>P</i> $\bar{1}$	<i>P</i> $\bar{1}$
<i>a</i> /Å	12.1855(6)	12.1674(5)	12.2378(6)	10.8792(6)	12.2288(5)	12.1075(7)
<i>b</i> /Å	8.0054(4)	7.9501(3)	12.5947(8)	14.3457(8)	12.4841(5)	12.4960(8)
<i>c</i> /Å	25.6608(12)	25.4391(10)	16.5103(8)	14.9616(8)	16.4978(7)	16.3917(10)
α /°	90	90	87.8249(10)	75.8170(10)	88.3160(10)	87.9649(9)
β /°	101.7220(10)	101.5860(10)	69.1710(09)	72.9120(9)	69.2430(9)	69.2030(10)
γ /°	90	90	70.7700(10)	73.8340(10)	70.7320(10)	70.8010(10)
<i>V</i> /Å ³	2451.0(2)	2410.64(16)	2236.69(19)	2109.6(2)	2212.28(16)	2180.2(2)
<i>Z</i>	4	4	2	2	2	2
<i>D</i> _{calcd} /g cm ⁻³	1.937	1.984	1.703	1.802	1.744	1.759
<i>T</i> /K	293(2)	293(2)	293(2)	293(2)	293(2)	173(2)
<i>F</i> (000)	1408	1420	1150	1138	1138	1156
μ /mm ⁻¹	2.771	3.199	2.368	3.268	2.819	2.677
θ rang/°	2.58–25.00	2.59–25.00	2.64–25.00	2.75–25.00	2.29–25.00	2.66–25.00
Reflections measured	11 552	11 512	11 182	10 307	10 815	10 697
Reflections used	4302	4239	7712	7191	7565	7448
Parameters	343	343	577	574	577	578
<i>R</i> ^a (<i>I</i> > 2 σ (<i>I</i>))	<i>R</i> ₁ = 0.0181 <i>wR</i> ₂ = 0.0431	<i>R</i> ₁ = 0.0184 <i>wR</i> ₂ = 0.0430	<i>R</i> ₁ = 0.0330 <i>wR</i> ₂ = 0.0781	<i>R</i> ₁ = 0.0272 <i>wR</i> ₂ = 0.0607	<i>R</i> ₁ = 0.0234 <i>wR</i> ₂ = 0.0599	<i>R</i> ₁ = 0.0198 <i>wR</i> ₂ = 0.0523
<i>R</i> ^a (all data)	<i>R</i> ₁ = 0.0216 <i>wR</i> ₂ = 0.0447	<i>R</i> ₁ = 0.0223 <i>wR</i> ₂ = 0.0446	<i>R</i> ₁ = 0.0447 <i>wR</i> ₂ = 0.0848	<i>R</i> ₁ = 0.0369 <i>wR</i> ₂ = 0.0649	<i>R</i> ₁ = 0.0267 <i>wR</i> ₂ = 0.0635	<i>R</i> ₁ = 0.0213 <i>wR</i> ₂ = 0.0532
<i>S</i>	1.083	1.047	1.026	1.007	1.028	1.023

$$^a R_1 = \sum \|F_o\| - |F_c| / \sum \|F_o\|, wR_2 = [\sum [w(F_o^2 - F_c^2)^2] / \sum [w(F_o^2)^2]]^{1/2}, w = 1 / [\sigma^2(F_o^2) + (mP)^2 + nP], \text{ where } P = (F_o^2 + 2F_c^2) / 3.$$

for the cyanate derivatives **2a–c** revealed strong bands at 2257, 2256 and 2251 cm⁻¹ assigned to the OCN⁻ group. For **3a–e**, bands around 2090 cm⁻¹ revealed the presence of the SCN⁻ ligand. Both groups of compounds exhibited strong absorptions at 1455–1458 and 1309–1317 cm⁻¹ typical for bidentate NO₃⁻ groups.

Structural studies

Cyanate (OCN⁻) complexes. Single-crystal X-ray diffraction studies were performed on cyanate complexes **2a** and **2b**. The two compounds are isostructural and crystallize in the monoclinic space group *P*2₁/*c*. Spectroscopic data supports the proposal that **2c** has a similar structure to those of **2a** and **2b**. Crystallographic details are provided in Table 1 and key bond lengths and angles are given in Tables 2 and 3, respectively. The 1D framework structure of these materials consists of dinuclear ZnLnLn units linked by OCN⁻ groups in a zig-zag chain. Views of the ZnLaLOCN unit and the 1D polymeric structure in **2a** are shown in Fig. 1 and 2, respectively. The OCN⁻ groups bridge the (LZnLa) moieties *via* coordination of the nitrogen atom to Zn and the oxygen to La, as expected from the hard/soft donor acceptor properties of the ligand and the 3d and 4f metals. Each Zn(II) ion has a five-coordinate distorted square pyramidal geometry composed of the inner N₂O₂ core of the Schiff base ligand with the N atom from OCN⁻ occupying the apical position. The Ln(III) ions are ten-coordinate being bound only to O atoms, four from the Schiff base, four from two bidentate NO₃⁻ groups, one from the OCN⁻ group and one from a water molecule. The zig-zag chain like structure can be compared to that observed in the heterobimetallic 3d–4f species [CuL'Pr(NO₃)₂(IN)]_∞ (H₂L' = *N,N'*-bis (3-methoxy-salicylidene)propylene-1,3-diamine, INH = isonicotinic acid),⁹ in

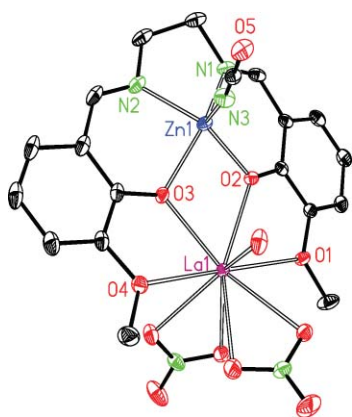
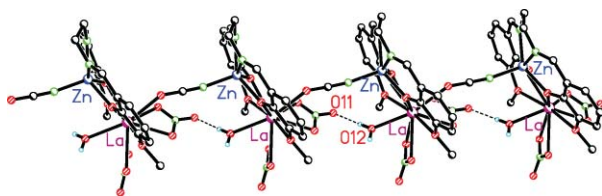
Table 2 Selected bond lengths (Å) and angles (°) for complex **2a**. Symmetry operator (*x*, 1 + *y*, *z*) generates equivalent atoms marked with “#”

Bond lengths/Å			
La(1)–O(3)	2.4483(16)	La(1)–O(2)	2.4737(15)
La(1)–O(12)	2.4937(19)	La(1)–O(5)#	2.5769(18)
La(1)–O(9)	2.6028(18)	La(1)–O(10)	2.6430(19)
La(1)–O(7)	2.6725(18)	La(1)–O(6)	2.682(2)
La(1)–O(1)	2.6835(16)	La(1)–O(4)	2.8533(17)
Zn(1)–N(1)	2.043(2)	Zn(1)–N(2)	2.081(2)
Zn(1)–N(3)	1.968(2)	Zn(1)–O(2)	2.0063(16)
Zn(1)–O(3)	2.0723(17)		
Bond angles/°			
O(3)–La(1)–O(1)	124.84(5)	O(3)–La(1)–O(2)	65.71(5)
O(3)–La(1)–O(4)	57.81(5)	O(2)–La(1)–O(1)	60.01(5)
O(1)–La(1)–O(4)	171.68(6)	O(2)–La(1)–O(4)	120.30(5)
O(2)–Zn(1)–O(3)	81.78(6)	O(2)–Zn(1)–N(1)	90.39(8)
O(2)–Zn(1)–N(2)	141.27(8)	N(1)–Zn(1)–O(3)	146.26(8)
O(3)–Zn(1)–N(2)	86.56(8)	N(1)–Zn(1)–N(2)	79.23(9)

which the N atom of the IN⁻ anion selectively coordinates to the relatively soft Cu ion while the two O atoms bind to the harder Pr(III) ions giving a 2D layer network. The 1D chain structures of **2a** and **2b** appear to be also reinforced by hydrogen bonded interactions between a proton of the coordinated H₂O molecule and one oxygen atom from a NO₃⁻ group on an adjacent [LZnLn] unit (Fig. 2). The short O(H₂O)⋯O(NO₃⁻) distances here are 2.865(5) Å (**2a**) and 2.881(5) Å (**2b**). The metrical parameters within the [LZnLn] cores of **2a,b** all fall within normal limits.

Table 3 Selected bond lengths (Å) and angles (°) for complex **2b**. Symmetry operator ($x, 1 + y, z$) generates equivalent atoms marked with “#”

Bond lengths/Å			
Nd(1)–O(3)	2.3862(17)	Nd(1)–O(2)	2.4141(16)
Nd(1)–O(12)	2.4346(19)	Nd(1)–O(5)	2.5359(19)
Nd(1)–O(11)#	2.5373(19)	Nd(1)–O(6)	2.5701(19)
Nd(1)–O(8)	2.610(2)	Nd(1)–O(9)	2.6222(19)
Nd(1)–O(1)	2.6353(17)	Nd(1)–O(4)	2.8883(18)
Zn(1)–O(2)	2.0042(16)	Zn(1)–O(3)	2.0738(18)
Zn(1)–N(1)	2.046(2)	Zn(1)–N(2)	2.075(2)
Zn(1)–N(3)	1.966(2)		
Bond angles/°			
O(3)–Nd(1)–O(1)	127.38(6)	O(3)–Nd(1)–O(2)	67.22(6)
O(3)–Nd(1)–O(4)	58.02(6)	O(2)–Nd(1)–O(1)	61.08(5)
O(1)–Nd(1)–O(4)	169.09(6)	O(2)–Nd(1)–O(4)	121.07(5)
O(2)–Zn(1)–O(3)	81.31(7)	O(2)–Zn(1)–N(1)	90.30(8)
O(2)–Zn(1)–N(2)	140.85(8)	N(1)–Zn(1)–O(3)	145.95(8)
O(3)–Zn(1)–N(2)	86.58(9)	N(1)–Zn(1)–N(2)	79.32(10)

**Fig. 1** Perspective view of **2a**. H atoms are omitted for clarity. Thermal ellipsoids are drawn at the 25% probability level.**Fig. 2** Hydrogen bonded interactions in **2a**. (O...O = 2.865 Å).

Thiocyanate (SCN⁻) complexes. The use of ammonium thiocyanate (NH₄SCN) instead of KOCN under similar reaction conditions to those used for the preparation of **2a–c** results in the formation of trinuclear complexes of general formula [Zn₂LnL₂(NO₃)(SCN)₂] (**3a–e**). Interestingly, since the S atom in SCN⁻ is much softer than the N atom in OCN⁻, it does not coordinate with the hard Ln³⁺ ions in series 3. As a result, series 3 do not show the 1D framework structures found in series 2. Complexes **3b–e** have been characterized by single-crystal X-ray diffraction studies and crystallographic details for these complexes are provided in Table 1. Key bond lengths and angles are in Tables 4–7, respectively. Compounds **3b**, **3d** and **3e** are isostructural and crystallize in the monoclinic space group $P\bar{1}$.

Table 4 Selected bond lengths (Å) and angles (°) for complex **3b**

Bond lengths/Å			
Nd(1)–O(3)	2.420(3)	Nd(1)–O(6)	2.434(3)
Nd(1)–O(2)	2.439(3)	Nd(1)–O(7)	2.448(3)
Nd(1)–O(10)	2.517(3)	Nd(1)–O(4)	2.591(3)
Nd(1)–O(9)	2.637(4)	Nd(1)–O(1)	2.678(3)
Nd(1)–O(8)	2.739(3)	Nd(1)–O(5)	2.805(3)
O(2)–Zn(1)	2.017(3)	O(3)–Zn(1)	2.076(3)
N(5)–Zn(1)	1.982(4)	N(1)–Zn(1)	2.088(4)
N(2)–Zn(1)	2.044(4)	O(6)–Zn(2)	2.042(3)
O(7)–Zn(2)	2.016(3)	N(3)–Zn(2)	2.085(4)
N(4)–Zn(2)	2.036(4)	N(6)–Zn(2)	1.961(4)
Bond angles/°			
O(3)–Nd(1)–O(2)	65.04(9)	O(3)–Nd(1)–O(4)	61.69(9)
O(2)–Nd(1)–O(4)	120.28(10)	O(3)–Nd(1)–O(1)	123.68(9)
O(2)–Nd(1)–O(1)	59.06(9)	O(4)–Nd(1)–O(1)	149.34(11)
O(2)–Zn(1)–N(2)	151.23(14)	O(2)–Zn(1)–O(3)	79.31(11)
N(2)–Zn(1)–O(3)	87.54(13)	O(2)–Zn(1)–N(1)	89.14(14)
N(2)–Zn(1)–N(1)	79.44(16)	O(3)–Zn(1)–N(1)	129.09(14)
O(7)–Zn(2)–N(4)	90.14(13)	O(7)–Zn(2)–O(6)	77.78(11)
N(4)–Zn(2)–O(6)	142.43(13)	O(7)–Zn(2)–N(3)	138.80(13)
N(4)–Zn(2)–N(3)	80.22(15)	O(6)–Zn(2)–N(3)	85.85(14)

Table 5 Selected bond lengths (Å) and angles (°) for complex **3c**

Bond lengths/Å			
Er(1)–O(3)	2.249(2)	Er(1)–O(7)	2.279(2)
Er(1)–O(6)	2.296(3)	Er(1)–O(2)	2.318(2)
Er(1)–O(10)	2.407(3)	Er(1)–O(9)	2.414(3)
Er(1)–O(1)	2.498(2)	Er(1)–O(4)	2.613(2)
Er(1)–O(8)	2.780(3)	N(1)–Zn(1)	2.062(4)
N(2)–Zn(1)	2.033(4)	N(3)–Zn(1)	1.958(4)
O(2)–Zn(1)	2.022(3)	O(3)–Zn(1)	2.009(3)
N(4)–Zn(2)	2.044(3)	N(5)–Zn(2)	2.080(3)
N(6)–Zn(2)	1.951(3)	O(6)–Zn(2)	2.061(2)
O(7)–Zn(2)	2.036(3)		
Bond angles/°			
O(3)–Er(1)–O(1)	126.55(9)	O(3)–Er(1)–O(2)	66.40(9)
O(3)–Er(1)–O(4)	62.75(9)	O(2)–Er(1)–O(1)	63.24(8)
O(1)–Er(1)–O(4)	159.05(9)	O(2)–Er(1)–O(4)	129.13(9)
O(3)–Zn(1)–N(2)	90.19(14)	O(3)–Zn(1)–O(2)	76.70(10)
O(3)–Zn(1)–N(1)	149.86(13)	O(2)–Zn(1)–N(2)	130.66(13)
N(2)–Zn(1)–N(1)	81.32(17)	O(2)–Zn(1)–N(1)	87.03(13)
O(7)–Zn(2)–O(6)	80.16(10)	O(7)–Zn(2)–N(4)	128.17(12)
O(7)–Zn(2)–N(5)	86.80(12)	N(4)–Zn(2)–O(6)	89.77(11)
O(6)–Zn(2)–N(5)	153.01(12)	N(4)–Zn(2)–N(5)	79.84(13)

Compound **3c** has a disordered water in the lattice and has a different unit cell from the others. The central cores of these molecules contain two Zn(II) ions bound by the inner N₂O₂ cores of two Schiff base units (Fig. 3). Each Zn(II) ion is five coordinate and has a distorted square pyramidal geometry with the apical position occupied by the N atom of an SCN⁻ anion. Although examples of SCN⁻ anions bridging two transition metals are known, in **3a–e** the S atoms remain uncoordinated and so a molecular species is formed instead of an infinite 1D polymer as in **2a–b**. The outer O₂O₂ binding sets of each ligand also coordinate the Ln(III) ions, which bear a bidentate nitrate group and are 10 coordinate. For each L ligand both phenolic O donors bridge the Zn(II) and Ln(III)

Table 6 Selected bond lengths (Å) and angles (°) for complex **3d**

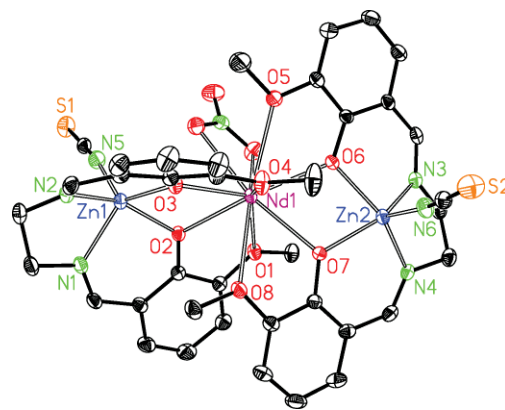
Bond lengths/Å			
O(1)–Tb(1)	2.701(2)	O(2)–Tb(1)	2.373(2)
O(3)–Tb(1)	2.3619(19)	O(4)–Tb(1)	2.844(2)
O(5)–Tb(1)	2.538(2)	O(6)–Tb(1)	2.3384(19)
O(7)–Tb(1)	2.3623(19)	O(8)–Tb(1)	2.665(2)
O(9)–Tb(1)	2.457(2)	O(10)–Tb(1)	2.590(3)
N(1)–Zn(1)	2.038(3)	N(2)–Zn(1)	2.075(3)
N(3)–Zn(1)	1.960(3)	O(2)–Zn(1)	2.0158(19)
O(3)–Zn(1)	2.043(2)	O(6)–Zn(2)	2.0731(19)
O(7)–Zn(2)	2.0153(19)	N(4)–Zn(2)	2.050(3)
N(5)–Zn(2)	2.082(3)	N(6)–Zn(2)	1.974(3)
Bond angles/°			
O(3)–Tb(1)–O(2)	64.22(7)	O(3)–Tb(1)–O(1)	121.00(7)
O(2)–Tb(1)–O(1)	59.63(7)	O(3)–Tb(1)–O(4)	57.58(7)
O(2)–Tb(1)–O(4)	115.14(7)	O(1)–Tb(1)–O(4)	138.55(8)
O(2)–Zn(1)–N(1)	90.32(9)	O(2)–Zn(1)–O(3)	76.65(8)
N(1)–Zn(1)–O(3)	142.84(10)	O(2)–Zn(1)–N(2)	137.64(9)
N(1)–Zn(1)–N(2)	80.28(11)	O(3)–Zn(1)–N(2)	86.32(9)
O(7)–Zn(2)–N(4)	150.28(10)	O(7)–Zn(2)–O(6)	77.84(8)
N(4)–Zn(2)–O(6)	87.58(9)	O(7)–Zn(2)–N(5)	89.44(9)
N(4)–Zn(2)–N(5)	79.22(11)	O(6)–Zn(2)–N(5)	127.91(9)

Table 7 Selected bond lengths (Å) and angles (°) for complex **3e**

Bond lengths/Å			
Eu(1)–O(6)	2.3734(15)	Eu(1)–O(7)	2.3984(15)
Eu(1)–O(2)	2.4003(15)	Eu(1)–O(3)	2.4061(15)
Eu(1)–O(9)	2.4718(17)	Eu(1)–O(5)	2.5517(16)
Eu(1)–O(10)	2.6131(18)	Eu(1)–O(8)	2.6596(15)
Eu(1)–O(4)	2.6991(16)	Eu(1)–O(1)	2.7672(17)
N(1)–Zn(1)	2.078(2)	N(2)–Zn(1)	2.0300(19)
N(3)–Zn(1)	1.965(2)	O(2)–Zn(1)	2.0384(16)
O(3)–Zn(1)	2.0208(15)	N(4)–Zn(2)	2.0468(19)
N(5)–Zn(2)	2.083(2)	N(6)–Zn(2)	1.979(2)
O(6)–Zn(2)	2.0769(15)	O(7)–Zn(2)	2.0137(15)
Bond angles/°			
O(2)–Eu(1)–O(3)	63.22(5)	O(2)–Eu(1)–O(4)	120.11(5)
O(3)–Eu(1)–O(4)	59.33(5)	O(2)–Eu(1)–O(1)	58.46(5)
O(3)–Eu(1)–O(1)	115.41(5)	O(4)–Eu(1)–O(1)	140.20(5)
O(3)–Zn(1)–N(2)	90.58(7)	O(3)–Zn(1)–O(2)	76.72(6)
N(2)–Zn(1)–O(2)	142.02(7)	O(3)–Zn(1)–N(1)	138.90(7)
N(2)–Zn(1)–N(1)	80.58(8)	O(2)–Zn(1)–N(1)	85.95(7)
O(7)–Zn(2)–N(4)	150.72(7)	O(7)–Zn(2)–O(6)	78.36(6)
N(4)–Zn(2)–O(6)	87.82(7)	O(7)–Zn(2)–N(5)	89.50(7)
N(4)–Zn(2)–N(5)	79.08(8)	O(6)–Zn(2)–N(5)	128.60(7)

ions and the separations between the metals is approximately 3.5 Å.

Conductivities of the compounds in dried and freshly distilled MeCN were all less than 1.0 $\mu\text{S cm}^{-1}$ demonstrating that they are all non-electrolytes in this solvent. The ^1H NMR spectra of La^{3+} complexes **2a** and **3a** in MeCN solution at room temperature are similar to that of the ligand, while the ^1H NMR spectra of Nd^{3+} compounds **2b** and **3b** show broad resonances ranging from around δ 11 to -4 ppm and are unchanged after one month. We have also probed the nature of these compounds in solution using high resolution ESI mass spectrometry studies. It would be reasonable to expect that in solution the 1D polymeric structures of the NCO derivatives break down into smaller,

**Fig. 3** Perspective view of **3b**. H atoms are omitted for clarity. Thermal ellipsoids are drawn at the 25% probability level.

more soluble units. The data for **2a** and **2b** are consistent with the presence of trimeric Zn_2Ln units in MeCN solution. Thus, for **2a** the two most prominent peak patterns correspond to $[\text{Zn}_2\text{LaL}(\text{L}-\text{CH}_2)(\text{OH})(\text{OCN})(\text{CH}_3\text{CN})(\text{H}_2\text{O})]^+$ (theoretical isotope for $\text{C}_{38}\text{H}_{40}\text{O}_{11}\text{N}_6\text{Zn}_2\text{La} = 1027.0364$, observed: 1027.0401) and $[\text{Zn}_2\text{La}(\text{L}-\text{CH}_2)_2(\text{OCN})_2(\text{CH}_3\text{CN})(\text{H}_2\text{O})]^+$ theoretical isotope: $\text{C}_{36}\text{H}_{33}\text{O}_{11}\text{N}_7\text{Zn}_2\text{La} = 1009.9846$, observed 1009.9890. Similar units are observed in the ESI-HRMS data for **2b**. In contrast the mass spectra (ESI-HRMS) of **3a** and **3b** in MeCN show the $[\text{M} - \text{NO}_3]^+$ fragment at m/z 1038.9685 (**3a**) (theoretical isotope: $\text{C}_{38}\text{H}_{36}\text{O}_8\text{N}_6\text{S}_2\text{Zn}_2\text{La} = 1038.9643$) and m/z 1014.9710 (**3b**) (theoretical isotope: $\text{C}_{38}\text{H}_{36}\text{O}_8\text{N}_6\text{S}_2\text{Zn}_2\text{Nd} = 1041.9696$). These observations indicate that in solution complexes **3a** and **3b** retain the trinuclear structure as found in the solid state.

Photophysical studies

The photophysical properties of the new complexes (series **2** and **3**) have been studied in acetonitrile solutions at room temperature and selected data are presented in Table 8. In order to study the influence of structural changes on photophysical properties, the

Table 8 Selected photophysical data^a for complexes **2a–c** and **3a–e**

	Absorption	Excitation	Emission
	$\lambda_{\text{max}}/\text{nm}[\log(\epsilon/\text{dm}^3 \text{ mol}^{-1} \text{ cm}^{-1})]$	$\lambda_{\text{exc}}/\text{nm}$	$\lambda_{\text{em}}/\text{nm}(\Phi_{\text{Zn-L}} \times 10^5, \tau)^b$
2a	265(4.35), 342(3.95)	361, 291	462 (19.2, 1.16 ns),
2b	264(4.29), 342(3.87)	363, 295	451 (2.65, 0.85 ns), 872 (1203 ns) ^c , 1067, 1356
2c	265(4.33), 340(3.89)	362, 291	461 (3.48, 0.94), 1529 ^d
3a	265(4.57), 344(4.23)	359, 294	489 (28.4, 1.55 ns)
3b	264(4.65), 344(4.17)	363, 292	464 (2.95, 1.14 ns), 884 (1246 ns), 1061, 1332
3c	264(4.59), 342(4.12)	383, 300	475 (6.42, 0.70), 1538
3d	264(4.68), 342(4.19)	367, 327	458 (5.40, 0.70 ns), 491, 545 (14.9 μs), 590, 624
3e	264(4.59), 342(4.12)	384, 305	459 (3.21, 0.95 ns)

^a Measurements were obtained in 2×10^{-5} M solution in CH_3CN .

^b Quantum yields of ligand-centered emissions were measured relative to quinine sulfate in 1.0 N H_2SO_4 ($\Phi_{\text{em}}=0.55$). ^c The quantum yield of the NIR luminescence could not be determined due to limitations of the instrumentation. ^d The lifetime of the NIR luminescence of the Er^{3+} compounds could not be measured due to limitations of the instrumentation.

luminescence properties of the bimetallic precursors (series **1**) are also included here. As illustrated in Fig. 4 for Ln = Nd (**1b**, **2b**, **3b**) the UV-vis absorption spectra of **2a–c** and **3a–e** are similar to those of the corresponding heterobimetallic nitrate based precursors [ZnLnL(H₂O)(NO₃)₃] (**1a–e**). Absorptions in the 250–400 nm range are attributed to π - π^* transitions of the Schiff base ligand.

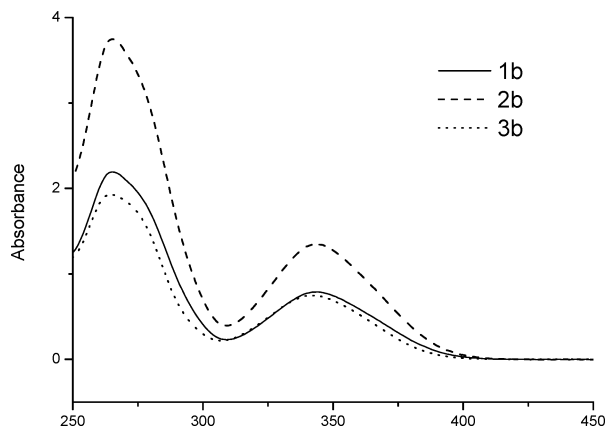


Fig. 4 Absorption spectra of **1b**, **2b** and **3b** in acetonitrile at room temperature. ($c = 2 \times 10^{-5}$ M)

Nd (1b, 2b, 3b). For the complexes **1–3b** containing Nd(III), excitation of the Schiff base chromophore in the 292–367 nm range gave rise to the characteristic emissions of the trivalent Nd³⁺ ions in the NIR region. (Fig. 5 and 6) The emission at 872 nm is assigned to the ${}^4F_{3/2} \rightarrow {}^4I_{9/2}$ transition while those at 1064 and 1334 nm are due to the ${}^4F_{3/2} \rightarrow {}^4I_{11/2}$, and ${}^4F_{3/2} \rightarrow {}^4I_{13/2}$ transitions, respectively. Meanwhile, a broad ligand-centered (antenna) emission in visible region at near 457 nm was found in each complex (Table 8). For these three Nd³⁺ complexes, the excitation spectra monitored at the NIR emission peaks are similar to those monitored at the ligand-centered emissions, indicating the energy transfer from the antenna (Zn-L) to Nd³⁺ ions takes place.

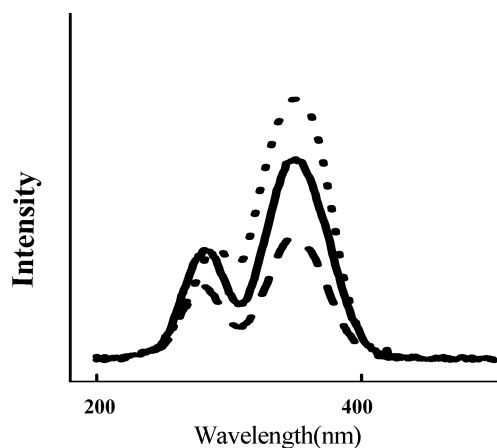


Fig. 5 Excitation spectra of **1b** (—), **2b** (---) and **3b** (···) in acetonitrile at room temperature. ($c = 2 \times 10^{-5}$ M).

Er (1c, 2c, 3c). As shown in Fig. 6, for the Er(III) containing complexes, **1–3c**, a relatively broad and weaker emission band (relative to **2a–c**) at 1538 nm, assigned to the ${}^4I_{13/2} \rightarrow {}^4I_{15/2}$

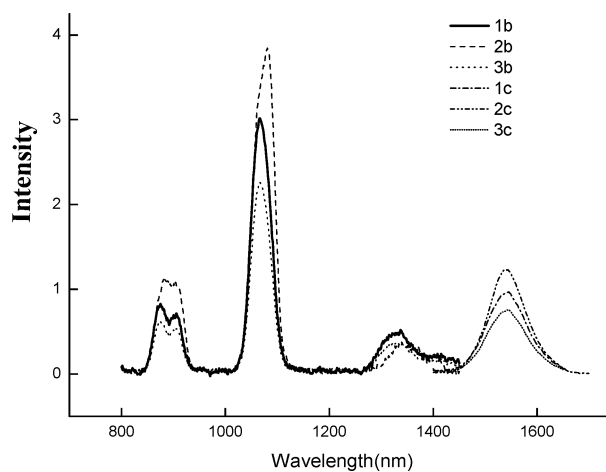


Fig. 6 NIR emission spectra of **1–3b** and **1–3c** in acetonitrile at room temperature with the same absorbance value at the excitation wavelength of 350 nm.

transition, is observed on excitation of the complexes at 350 nm where **1–3c** and **1–3b** have the same absorbance values. This is in agreement with literature data for Nd(III) vs. Er(III).^{10,11}

Tb (1d, 3d). Excitation of the ligand centered absorption bands in both complexes result in typical visible emission bands for the Tb³⁺ ion (${}^5D_4 \rightarrow {}^7F_n$ transitions, $n = 6, 5, 4$ and 3). The excitation and emission spectra of **3d** are shown in Fig. 7. The strongest emission is centered around 545 nm and is assigned to the sensitive ${}^5D_4 \rightarrow {}^7F_5$ transition.

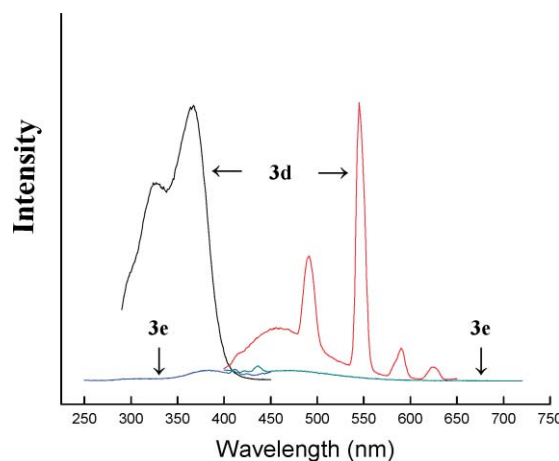


Fig. 7 Excitation and emission spectra of **3d** and **3e** in acetonitrile at room temperature. ($c = 2 \times 10^{-5}$ M).

Eu (3e). In contrast to the observable emission spectra for the other complexes, excitation of **3e** at the ligand centered absorption bands did not result in a corresponding Eu(III) centered transition (${}^6D_4 \rightarrow {}^7F_j$, $j = 0, 1, 2, 3$ and 4 , Fig. 7). One explanation for this is that there is a deactivation pathway that involves a charge-transfer process from the Zn-L excited state to the Eu³⁺ ion. The measured redox potential (E_{red}) for the Eu³⁺ \rightarrow Eu²⁺ couple in **3e** is -0.504 V vs. Ag/AgCl reference electrode. The excited-state oxidation potential of Zn-Schiff-base is estimated to be ${}^1E_{\text{ox}}^* = -1.94$ V, which is obtained from the ground state oxidation potential ${}^1E_{\text{ox}}$ (0.82 V vs. Ag/AgCl reference electrode,

measured by cyclic voltammetry) and its singlet state energy ${}^1E_{00}$ (2.76 V, calculated with ${}^1E_{00} = hc/\lambda_{em}e$, $\lambda_{em} = 449$ nm) according to the equation ${}^1E_{ox}^* = {}^1E_{ox} - {}^1E_{00}$.¹² Thus, the possible mechanism of quenching is the electron transfer from excited state Zn-L to the Eu^{3+} ion. While the reduction potential of Tb^{3+} is too negative making this electron transfer quenching far less likely in the compound **3d**. (e.g. $E_{red} = -3.658$ V vs. NHE. We could not measure the E_{red} of Tb^{3+} in **3d** due to the limitations with our instrumentation.)

All complexes exhibit a broad ligand-centered (antenna) emission in the visible region near to 460 nm, indicating that the ligand-to-metal energy transfers take place incompletely. The quantum yields and lifetimes of these ligand-centered emissions are shown in Table 8. As expected, the quantum yield of **2a** and **3a** which contain non-emitting La^{3+} ions are much higher (more than 4 times) than those of other luminescent complexes.

The overall luminescence quantum yield (Φ_{tot}) of the Ln^{3+} ion is given by eqn (1):¹³

$$\Phi_{tot} = \eta_{sens} \times \Phi_{Ln} = \eta_{sens} \times (\tau_{obs}/\tau_0) \quad (1)$$

where η_{sens} , Φ_{Ln} , τ_{obs} and τ_0 are ligand sensitization efficiency, the intrinsic quantum yield of the lanthanide itself, the observed lifetime and natural lifetime, respectively.

The luminescent decay curves obtained from time-resolved luminescence experiments can be fitted mono-exponentially with time constants in the microsecond range. The lifetimes of the NIR luminescence of Nd^{3+} complexes are shown in Table 8. The overall NIR luminescence quantum yields of Nd^{3+} and Er^{3+} complexes could not be measured directly due to limitations with our instrumentation. However, the intrinsic quantum yields Φ_{Ln} can be estimated from eqn (1). For example, the natural lifetimes (τ_0) are 0.25 ms and 14 ms for Nd^{3+} and Er^{3+} ions, respectively.¹⁰ This gives values of the intrinsic quantum yields (Φ_{Ln}) for **2b** and **3b** of 0.0048 and 0.0050, respectively. For the Tb^{3+} complex **3d**, although the ligand-centered (antenna) and Tb^{3+} ion emissions overlap together in the visible region, it is possible to deconvolute them by using Gaussian using the ORIGIN program. The overall lanthanide luminescence quantum yield for **3d** is 5.3×10^{-5} .

We were interested in the influence of structural differences between bimetallic precursors (series **1**) and trinuclear compounds (series **3**) on their photophysical properties. With the same absorbance value at 350 nm, the relative emission areas in the NIR region for the Nd and Er complexes **3b** : **1b** and **3c** : **1c** in MeCN were 1.29 and 1.17, respectively (Fig. 7), indicating **3b** and **3c** have stronger NIR emissions than **1b** and **1c**, respectively. This difference in luminescence properties may be due to the different Ln^{3+} environments in the complexes. In series **3**, each Ln^{3+} ion is encapsulated by two Schiff-base ligands which make it less exposed to possible interactions with solvent molecules which could quench the luminescence.⁴ Meaningful comparisons with solution photophysical properties of the 1D polymeric compound **2a-c** can not be made since these materials have a different composition in solution, as noted above.

Experimental

Starting materials and solvents were used as purchased without further purification unless otherwise stated. The ligand H_2L and the precursor **3d-4f** heterobimetallic complexes **1a-e** were pre-

pared according to literature methods.^{7a,7i} Elemental analyses (C, H, N) were performed on a Perkin-Elmer 240C elemental analyzer. Infrared spectra (KBr pellets) were recorded on a PerkinElmer spectrum 100 FT-IR spectrometer. UV-vis absorption spectra were obtained on a Cary 300 UV spectrophotometer. Steady-state visible fluorescence and PL excitation spectra, on a Photon Technology International (PTI) Alphascan spectrofluorometer, and visible decay spectra, on a pico-N₂ laser system (PTI Time Master) with $\lambda_{ex} = 337$ nm. NIR emission was recorded by PTI QM4 spectrofluorometer with a PTI QM4 Near-Infrared InGaAs detector. Cyclic voltammetry of the Zn-Schiff-base was performed on a CHI 630C electrochemical workstation with a three-electrode in DMSO using $[\text{Bu}_4\text{N}][\text{PF}_6]$ (0.1 M) as the supporting electrolyte with a scan rate of 0.150 V s^{-1} . The solution was deoxygenated by nitrogen gas prior to measurement. Cyclic voltammetry was conducted with a glassy carbon electrode, a platinum wire as the auxiliary electrode, and an Ag/AgCl (saturated) reference electrode at room temperature. The working electrode was polished with $0.03 \mu\text{m}$ aluminium and was subjected to ultrasonic radiation for 1 min before each experiment.

Synthesis

General procedure for the preparation of complexes 2a-c. The precursor complex $[\text{ZnLnL}(\text{H}_2\text{O})(\text{NO}_3)_3]$ (0.1 mmol) was dissolved in acetonitrile (30 mL) and potassium cyanate (0.1 mmol) was added with stirring. The mixture was heated under reflux (2 h) before being cooled to room temp. The resultant solution was filtered and solvent from the filtrate allowed to evaporate slowly at room temperature. The product was isolated by filtration after several days.

$[\text{ZnLaL}(\text{NO}_3)_2(\text{H}_2\text{O})(\text{OCN})]_{\infty}$ (2a**).** 71.6 mg of **1a** was used. 53 mg pale yellow crystals of **2a** were obtained (yield: 70%). ESI-HRMS: m/z 1027.0401 $[\text{Zn}_2\text{LaL}(\text{L-CH}_2)(\text{OH})(\text{OCN})(\text{CH}_3\text{CN})(\text{H}_2\text{O})]^+$ (theoretical isotope: $\text{C}_{38}\text{H}_{40}\text{O}_{11}\text{N}_6\text{Zn}_2\text{La} = 1027.0364$). ${}^1\text{H}$ NMR [400 MHz, $\text{CD}_3\text{CN}/\text{DMSO-d}_6$ (v/v = 5 : 1)] δ/ppm : 8.61 (1 H), 8.48 (1 H), 7.23 (1 H), 7.15 (1 H), 7.09 (1 H), 7.01 (1 H), 6.85 (1 H), 6.80 (1 H), 3.99 (5 H), 3.78 (5 H). IR (cm^{-1} , KBr): 3411 (m), 2257 (s), 1648 (s), 1454 (s), 1384 (s), 1314 (m), 1280 (m), 1239 (w), 1221 (m), 1074 (w), 1038 (w), 957 (w), 848 (w), 735 (m), 639 (w). Element analysis: calculated for $\text{C}_{19}\text{H}_{20}\text{LaN}_5\text{O}_{12}\text{Zn}$: C 31.93, H 2.82, N 9.80. Found: C 32.04, H 2.77, N 9.97.

$[\text{ZnNdL}(\text{NO}_3)_2(\text{H}_2\text{O})(\text{OCN})]_{\infty}$ (2b**).** 72 mg **1b** was used, 47 mg pale blue crystals were obtained (yield: 65.1%). ESI-HRMS: m/z 1016.0225 $[\text{Zn}_2\text{Nd}(\text{L-CH}_2)_2(\text{OCN})_2(\text{OH})(\text{CH}_3\text{CN})(\text{H}_2\text{O})]^+$ (theoretical isotope: $\text{C}_{37}\text{H}_{38}\text{O}_{11}\text{N}_6\text{Zn}_2\text{Nd} = 1016.0259$). ${}^1\text{H}$ NMR (400 MHz; CD_3CN) δ/ppm : 11.59 (2 H), 8.00 (2 H), 7.98 (4 H), 4.92 (2 H), 0.36 (2 H), -4.43 (6 H). IR (cm^{-1} , KBr): 3428 (m), 2256 (s), 1649 (s), 1471 (w), 1455 (s), 1441 (w) 1384 (s), 1317 (s), 1279 (s), 1222 (s), 1170 (w), 1075 (m), 1038 (w), 958 (m), 848 (w), 735 (m), 640 (w). Element analysis: calculated for $\text{C}_{19}\text{H}_{20}\text{N}_5\text{NdO}_{12}\text{Zn}$: C 31.69, H 2.80, N 9.73. Found: C 31.81, H 2.70, N 9.80.

$[\text{ZnErL}(\text{NO}_3)_2(\text{H}_2\text{O})(\text{OCN})]_{\infty}$ (2c**).** 74.5 mg **1c** was used and 44 mg yellow crystals were obtained (yield: 59.4%). IR (cm^{-1} , KBr): 3428 (m), 2251 (s), 1649 (s), 1471 (w), 1455 (s), 1441 (w) 1384 (s), 1317 (s), 1279 (s), 1222 (s), 1170 (w), 1075 (m), 1038 (w), 958 (m), 848 (w), 735 (m), 640 (w). Element analysis: calculated for

$C_{19}H_{20}ErN_5O_{12}Zn$: C 30.71, H 2.71, N 9.43. Found: C 32.09, H 2.69, N 9.58.

General synthesis procedure for 3a–e. The precursor complex $[ZnLnL(H_2O)(NO_3)_3]$ (0.1 mmol) was dissolved in acetonitrile (20 mL) and ammonium thiocyanate (7.6 mg) was added with stirring. The mixture was heated under reflux (3 h) before being cooled to room temperature. The resultant solution was filtered and solvent from the filtrate allowed to evaporate slowly at room temperature. The product was isolated by filtration after several days.

$[Zn_2LaL_2(NO_3)(SCN)_2]$ (3a). 71.6 mg **1a** was used. A yellow solid of **2a** was obtained after two weeks. Yield: 45.2 mg (82%). ESI-HRMS: m/z 1038.9685 $[M - NO_3]^+$ (theoretical isotope: $C_{38}H_{36}O_8N_6S_2Zn_2La = 1038.9643$). 1H NMR [400 MHz, $CD_3CN/DMSO-d_6$ ($v/v = 5 : 1$)] δ/ppm : 8.41 (2 H), 7.06 (2 H), 7.01 (2 H), 6.82 (2 H), 3.76 (4 H + 6 H). IR (cm^{-1} , KBr): 3442 (m), 2088 (s), 1641 (s), 1605 (m), 1469 (s), 1459 (s), 1384 (s), 1279 (s), 1237 (m), 1218 (s), 1075 (m), 954 (m), 849 (m), 737 (s), 641 (m). Element analysis: calculated for $C_{38}H_{36}LaN_7O_{11}S_2Zn_2$: C 41.47, H 3.30, N 8.91. Found: C 41.52, H 3.32, N 8.89.

$[Zn_2NdL_2(NO_3)(SCN)_2] \cdot CH_3CN$ (3b). 72.2 mg **1b** was used and pale yellow crystals of **2b** were isolated two weeks later. Yield: 41.4 mg (75%). ESI-HRMS: m/z 1014.9710 $[M - NO_3]^+$ (theoretical isotope: $C_{38}H_{36}O_8N_6S_2Zn_2Nd = 1041.9696$). 1H NMR (400 MHz; $CD_3CN + DMSO-d_6$) δ/ppm : 11.00 (4 H), 7.74 (12 H), 4.77 (4 H), 0.54 (4 H), -4.07 (12 H). IR (cm^{-1} , KBr): 3435 (m), 2089 (s), 1658 (s), 1642 (s), 1605 (m), 1554 (w), 1469 (s), 1458 (s), 1384 (s), 1332 (w), 1309 (w), 1280 (s), 1236 (m), 1217 (s), 1169 (w), 1099 (w), 1073 (m), 1036 (w), 954 (m), 848 (m), 737 (s), 638 (m). Element analysis: calcd for $C_{40}H_{39}N_8NdO_{11}S_2Zn_2$: C 41.89, H 3.43, N 9.77. Found: C 41.81, H 3.50, N 9.69.

$[Zn_2ErL_2(NO_3)(SCN)_2] \cdot H_2O$ (3c). 74.5 mg **1c** was used to give yellow crystals of **2c** one month later. Yield: 37.4 mg (68%). IR (cm^{-1} , KBr): 3435 (m), 2081 (s), 1635 (s), 1606 (m), 1557 (w), 1522 (m), 1470 (s), 1458 (s), 1384 (s), 1278 (s), 1267 (s), 1243 (m), 1220 (s), 1079 (m), 955 (m), 849 (m), 781 (w), 738 (m). Element analysis: calcd for $C_{38}H_{38}N_7O_{12}S_2ErZn_2$: C 39.79, H 3.34, N 8.55. Found: C 40.76, H 3.29, N 9.44.

$[Zn_2TbL_2(NO_3)(SCN)_2] \cdot CH_3CN$ (3d). 73.6 mg **1d** was used and colourless crystals of **2d** were obtained after one month. Yield: 30.5 mg (53%). IR (cm^{-1} , KBr): 3436 (m), 2089 (s), 1658 (m), 1643 (s), 1562 (w), 1459 (s), 1470 (s), 1384 (s), 1282 (m), 1218 (s), 1074 (w), 955 (w), 848 (w), 737 (m), 638 (w). Element analysis: calcd for $C_{40}H_{39}N_8O_{11}S_2TbZn_2$: C 41.36, H 3.38, N 9.65. Found: C 41.05, H 3.31, N 9.21.

$[Zn_2EuL_2(NO_3)(SCN)_2] \cdot CH_3CN$ (3e). 73.0 mg **1e** was used to give dark red crystals of **2e** one month later. Yield: 48.1 mg (86%). IR (cm^{-1} , KBr): 3435 (m), 2089 (s), 1658 (m), 1643 (s), 1605 (m), 1555, 1470 (s), 1458 (s), 1384 (s), 1331 (w), 1313 (w), 1281 (s), 1217 (s), 1072 (m), 955 (m), 848 (m), 737 (m), 638 (w). Element analysis: calcd for $C_{40}H_{39}EuN_8O_{11}S_2Zn_2$: C 41.61, H 3.40, N 9.70. Found: C 41.31, H 3.35, N 9.26.

Conductivity measurements. The conductivities of the compounds in dried and freshly distilled acetonitrile were all less than

$1.0 \mu S cm^{-1}$ demonstrating that they are all non-electrolytes in this solvent.

X-Ray crystallography

Single crystals of **2b–e** and **3a–c** suitable for X-ray diffraction studies were mounted at the tip of a glass fiber for data collection. Intensity data were collected at 293 K (or 173 K for **3e**) on a Bruker AXS SMART 1000 CCD detector diffractometer using graphite-monochromated Mo-K α radiation ($\lambda = 0.71073 \text{ \AA}$). The collected frames were processed with the software SAINT,¹⁴ and an absorption correction was applied (SADABS)¹⁵ to the collected reflections. The structures of all compounds were solved by direct methods (SHELXTL)¹⁶ and refined against F^2 by full matrix least-squares analysis. All non-hydrogen atoms were refined anisotropically for these structures. Hydrogen atoms were generated in their idealized positions and allowed to ride on their respective parent carbon atoms. Crystal data collection and refinement parameters are given in Table 1, and selected bond distances and angles are in Tables 2–7.

Conclusions

This work demonstrates that cyanato bridged one dimensional 3d–4f polymeric or trinuclear 3d–4f–3d Schiff-base complexes with enhanced luminescent properties can be formed from the corresponding bimetallic precursors by self-assembly. Control of the functional linkage may be a potentially effective way to fine-tune the luminescent properties of such 3d–4f coordination complexes.

Acknowledgements

We thank Hong Kong Baptist University (FRG/06-07/II-16), the Hong Kong Research Grants Council (HKBU 202407), the Robert A. Welch Foundation (Grant F-816), the Texas Higher Education Coordinating Board (ARP 003658-0010-2006) and the Petroleum Research Fund, administered by the American Chemical Society (47014-AC5) financial support.

References

- (a) I. Hemmilä, T. Stahlberg and P. Mottram, *Bioanalytical Applications of Labeling Technologies*, Turku, Finland, 1994; (b) O. M. Yaghi, M. O'Keeffe and M. Kanatzidis, *J. Solid State Chem.*, 2000, **152**, 1.
- W. D. Jr. Horrocks and M. Albin, *Progress in Inorganic Chemistry*, John Wiley & Sons, New York, 1984.
- (a) A. Beeby, R. S. Dickins, S. Faulkner, D. Parker and J. A. G. Williams, *Chem. Commun.*, 1997, 1401; (b) S. I. Klink, G. A. Hebbink, L. Grave, F. C. J. M. van Veggel, D. N. Reinhoudt, L. H. Slooff, A. Polman and J. W. Hofstraat, *J. Appl. Phys.*, 1999, **86**, 1181; (c) A. Beeby, R. S. Dickins, S. FitzGerald, L. J. Govenlock, C. L. Maupin, D. Parker, J. P. Riehl, G. Siligardi and J. A. G. Williams, *Chem. Commun.*, 2000, 1183.
- N. Sabbatini, M. Guardigli and J. M. Lehn, *Coord. Chem. Rev.*, 1993, **123**, 201.
- (a) S. G.-P. Alison, A. K. Ishenkumba, J. P. W. Andrew and J. W. David, *Inorg. Chem.*, 1999, **38**, 1745; (b) L. J. Peter, J. A. Angelo, C. J. John, A. M. Jon, P. Elefteria, H. R. Leigh and D. W. Michael, *Inorg. Chem.*, 1997, **36**, 10; (c) K. Ohash, S. Yoshikawa, B. Akutsu, Y. Nakano and Y. Usui, *Anal. Sci.*, 1990, **6**, 827; (d) B. Alpha, J.-M. Lehn and G. Mathis, *Angew. Chem., Int. Ed. Engl.*, 1987, **26**, 266.
- (a) D. Imbert, M. Cantuel, J.-C. G. Bünzli, G. Bernardinelli and C. Piguet, *J. Am. Chem. Soc.*, 2003, **125**, 15698; (b) S. Torelli, D. Imbert, M. Cantuel, G. Bernardinelli, S. Delahaye, A. Hauser, J.-C. G. Bunzli

- and C. Piguet, *Chem.–Eur. J.*, 2005, **11**, 3228; (c) S. I. Klink, H. Keizer and F. C. J. M. van Veggel, *Angew. Chem., Int. Ed.*, 2000, **39**, 4319; (d) D. Guo, C.-Y. Duan, F. Lu, Y. Hasegawa, Q.-J. Meng and S. Yanagida, *Chem. Commun.*, 2004, 1486; (e) N. M. Shavaleev, L. P. Moorcraft, S. J. A. Pope, Z. R. Bell, S. Faulkner and M. D. Ward, *Chem. Commun.*, 2003, 1134; (f) N. M. Shavaleev, L. P. Moorcraft, S. J. A. Pope, Z. R. Bell, S. Faulkner and M. D. Ward, *Chem.–Eur. J.*, 2003, **9**, 5283; (g) P. B. Glover, P. R. Ashton, L. J. Childs, A. Rodger, M. Kercher, R. M. Williams, L. D. Cola and Z. Pikramenou, *J. Am. Chem. Soc.*, 2003, **125**, 9918; (h) H.-B. Xu, L.-X. Shi, E. Ma, L.-Y. Zhang, Q.-H. Wei and Z.-N. Chen, *Chem. Commun.*, 2006, 1601; (i) U. Casellato, P. Guerriero, S. Tamburini, S. Sitran and P. A. Vigato, *J. Chem. Soc., Dalton Trans.*, 1991, 2145.
- 7 (a) W.-K. Wong, H. Liang, W.-Y. Wong, Z. Cai, K.-F. Li and K.-W. Cheah, *New J. Chem.*, 2002, **26**, 275; (b) W.-K. Lo, W.-K. Wong, J.-P. Guo, W.-Y. Wong, K.-F. Li and K.-W. Cheah, *Inorg. Chim. Acta*, 2004, **357**, 4510; (c) X.-P. Yang, R. A. Jones, V. Lynch, M. M. Oye and A. L. Holmes, *Dalton Trans.*, 2005, 849; (d) X.-P. Yang and R. A. Jones, *J. Am. Chem. Soc.*, 2005, **127**, 7686; (e) W.-K. Wong, X.-P. Yang, R. A. Jones, J. H. Rivers, V. Lynch, W.-K. Lo, D. Xiao, M. M. Oye and A. L. Holmes, *Inorg. Chem.*, 2006, **45**, 4340; (f) X.-P. Yang, R. A. Jones, Q.-Y. Wu, M. M. Oye, W.-K. Lo, W.-K. Wong and A. L. Holmes, *Polyhedron*, 2006, **25**, 271; (g) W.-K. Lo, W.-K. Wong, W.-Y. Wong, J.-P. Guo, K.-T. Yeung, Y.-K. Cheng, X.-P. Yang and R. A. Jones, *Inorg. Chem.*, 2006, **45**, 9315; (h) X.-P. Yang, R. A. Jones, W.-K. Wong, M. M. Oye and A. L. Holmes, *Chem. Commun.*, 2006, 1836; (i) X. Q. Lü, W. Y. Bi, W. L. Chai, J. R. Song, a J. X. Meng, W. Y. Wong, W. K. Wong and R. A. Jones, *New J. Chem.*, 2008, **32**, 127; (j) X. Q. Lü, W. Y. Bi, W. L. Chai, J. R. Song, a J. X. Meng, W. Y. Wong, W. K. Wong, X.-P. Yang and R. A. Jones, *Polyhedron*, 2009, **28**, 27.
- 8 X. Y. Wang, Z. M. Wang and S. Gao, *Chem. Commun.*, 2008, 281.
- 9 R. Gheorghe, M. Andruh, A. Muller and M. Schmidtman, *Inorg. Chem.*, 2002, **41**, 5314.
- 10 S. I. Klink, L. Grave, D. N. Reinhoudt, F. C. J. M. van Veggel, M. H. Werts, F. A. J. Geurts and J. W. Hofstraat, *J. Phys. Chem. A*, 2000, **104**, 5457.
- 11 (a) N. M. Shavaleev, S. J. A. Pope, Z. R. Bell, S. Faulkner and M. D. Ward, *Dalton Trans.*, 2003808 and references therein; (b) T. Lazarides, G. M. Davies, H. Adams, C. Sabatini, F. Barigettetti, A. Barbieri, S. J. A. Pope, S. Faulkner and M. D. Ward, *Photochem. Photobiol. Sci.*, 2007, **6**, 1152; (c) T. Lazarides, T. L. Easun, C. Veyne-Marti, W. Z. Alsindi, M. W. George, N. Deppermann, C. A. Hunter, H. Adams and M. D. Ward, *J. Am. Chem. Soc.*, 2007, **129**, 4014; (d) G. M. Davies, S. J. A. Pope, H. Adams, S. Faulkner and M. D. Ward, *Inorg. Chem.*, 2005, **44**, 4656.
- 12 M. Asha Jhonsi and R. Renganathan, *Z. Phys. Chem.*, 2008, **222**, 1601.
- 13 J.-C. G. Bünzli, *Chem. Lett.*, 2009, **38**, 104.
- 14 *SAINT, Reference Manual* Siemens Energy and Automation, Madison, WI, 1994-1996.
- 15 G. M. Sheldrick, *SADABS, Empirical Absorption Correction Program* University of Göttingen, Göttingen, Germany, 1997.
- 16 G. M. Sheldrick, *SHELXTL, Reference Manual*, ver. 5.1; Siemens Energy and Automation, Madison, WI, 1997.